

Geophysical Research Letters®



RESEARCH LETTER

10.1029/2022GL100550

Correcting Systematic Bias in Climate Model Simulations in the Time-Frequency Domain

Cilcia Kusumastuti^{1,2} , Ze Jiang¹ , Rajeshwar Mehrotra¹ , and Ashish Sharma¹ 

¹Water Research Centre, School of Civil and Environmental Engineering, The University of New South Wales, Sydney, NSW, Australia, ²Department of Civil Engineering, Petra Christian University, Surabaya, Indonesia

Key Points:

- Systematic biases exist in the magnitude and frequency of climate events simulated by the models
- A continuous wavelet transform-based method for identifying and correcting biases in the time-frequency domain is presented
- Time series of Niño 3.4 sea surface temperature and Arctic sea-ice extent is used to demonstrate the usefulness of the approach

Correspondence to:

A. Sharma,
a.sharma@unsw.edu.au

Citation:

Kusumastuti, C., Jiang, Z., Mehrotra, R., & Sharma, A. (2022). Correcting systematic bias in climate model simulations in the time-frequency domain. *Geophysical Research Letters*, 49, e2022GL100550. <https://doi.org/10.1029/2022GL100550>

Received 26 JUL 2022
Accepted 9 SEP 2022

Abstract Systematic biases in General Circulation Model (GCM) simulations require some adjustment before their use in change assessment and adaptation management studies. GCM simulations of the Coupled Model Intercomparison Project 6, although outperform the previous generations of GCMs, exhibit persistent biases in magnitude, variability, and frequency across a range of variables of interest. Here, we propose a novel continuous wavelet-based bias correction (CWBC) approach to address such biases in the time-frequency domain. The correction focuses on the magnitude and frequency of the modeled time series, as interpreted via the time-varying spectrum ascertained using the continuous wavelet transform. The approach is applied to correct systematic biases in the time series of Niño 3.4 sea surface temperature and Arctic sea-ice extent. The application of CWBC successfully reproduces observed attributes in the bias-corrected time series of both climate variables for the current climate simulation along with providing a sensible projection for the future.

Plain Language Summary The latest generation of General Circulation Models outperforms older versions in simulating the current and future climate. However, biases in magnitude, frequency, variability, and persistence related characteristics still remain in model simulations. The nested time based and other frequency analysis-based bias correction approaches, for example, a fast Fourier transform or a discrete wavelet-based bias correction, offer a good alternative to correct the biases. However, they cannot capture the underlying components of climate variables in the non-dyadic spectrum. Keeping this in mind, we present here a continuous wavelet transform based bias correction approach to obtain the underlying information of climate variables at a finer spectrum resolution. The applications of continuous wavelet-based bias correction algorithm show remarkable improvement in the amplitude and frequency of two example datasets, namely, a Coupled Model Intercomparison Project 6 (CMIP6) sea surface temperature simulation and the ensemble mean of CMIP5 Arctic sea-ice extent simulations, for the current climate and more sensible correction for future climate simulations.

1. Introduction

With advances in computing power and an improved understanding of science, General Circulation Models (GCMs) keep improving with each generation to better mimic the observed climate (Beadling et al., 2020; Fan et al., 2020; Wang et al., 2021). At the same time, it is well accepted that model development constraints create persistent biases in simulations (Beadling et al., 2020), limiting direct use in on-ground adaptation studies focused on future climates (Bollasina & Ming, 2013; Mehrotra et al., 2014; Randall et al., 2007). This has resulted in many alternatives being proposed to address systematic model biases and forms the focus of the present study.

Most bias correction approaches in use are tailored to correct specific statistical attributes, for example, mean and standard deviation, cross-correlation coefficient, persistence (Johnson & Sharma, 2012; Mehrotra & Sharma, 2015; Nguyen et al., 2016), or to mimic the simulated probability distribution to observations using variations of the Quantile Matching (QM) approach (Haerter et al., 2011; Li et al., 2010; Teutschbein & Seibert, 2013; Wood et al., 2004). The QM is a popular alternative to correct distributional biases but is univariate as traditionally defined and ignores persistence and dependence biases. For climate model simulations to be used for water supply assessments, the representation of seasonal, annual, or over-the-year cycles that characterize observed physical phenomena needs consideration. For example, interannual rainfall variability in much of the world is largely a function of the Tropical Atlantic Sea Surface Temperature (TAV) and the El Niño-Southern Oscillation (ENSO) (Trauth et al., 2003). Inability to simulate these low-frequency variability modes in our climate may lead to an inaccurate estimation of the risk of water supply failure and impact planning and management decisions

© 2022 The Authors.

This is an open access article under the terms of the [Creative Commons Attribution-NonCommercial License](https://creativecommons.org/licenses/by-nc/4.0/), which permits use, distribution and reproduction in any medium, provided the original work is properly cited and is not used for commercial purposes.

(Johnson & Sharma, 2011; Mehrotra & Sharma, 2012). The importance of low-frequency variability bias in water resources applications has led to a suite of alternatives that correct for persistence across multiple time scales along with correcting for distributional bias (Johnson & Sharma, 2012; Mehrotra & Sharma, 2015; Ojha et al., 2013). The need for specifying nesting time-frames, while convenient to enable focus on both intra and inter-annual variability, limits the correction across the entire frequency spectrum. This has led to the development of rank space based and frequency analysis based bias correction approaches, for example, a three-dimensional bias correction (Mehrotra & Sharma, 2019) or fast Fourier transformation based bias correction (FBC) (Nguyen et al., 2016) or wavelet-based bias correction (WBC) (Kusumastuti et al., 2021), the latter having the added advantage of operating in the time-frequency space and enabling correction of time-dependent attributes (such as trend). WBC employs the strength of discrete wavelet transform to obtain the underlying trend in climate variables time series and is hereafter referred to as discrete wavelet-based bias correction (DWBC).

While the elegance of the DWBC arises from the use of the discrete wavelet transform (DWT), widely adopted for a range of applications in climatology (Abramovich et al., 2000; Adarsh & Janga Reddy, 2015; Jiang, Rashid, et al., 2021; Jiang, Sharma, & Johnson, 2021; Jiang et al., 2020; Lin, et al., 2019; Maheswaran & Khosa, 2012; Nourani et al., 2018; Sang et al., 2013), it limits application to variability over defined ranges of the spectrum, as one can focus only on dyadic frequency components. Given the importance of low-frequency variability in a range of applications, and the distinct possibility of it corresponding to the non-dyadic spectrum, the use of DWT may miss crucial information.

Considering this, we propose here an approach that is designed to extend existing time-frequency domain correction alternatives to non-dyadic frequencies. The approach is based on continuous wavelet transform (CWT) and is hereafter referred to as continuous wavelet-based bias correction (CWBC) approach. CWT has been used extensively for frequency analysis of climate variables (Brunner & Gilleland, 2020; Rashid et al., 2018; 2020) and also to observe the trend and periodicities of climate indicator, the Pacific Decadal Oscillation (Adamowski et al., 2009), to observe the power of Nino3 sea surface temperature (Torrence & Compo, 1998), to observe the trend in rainfall (Rashid et al., 2018, 2020) and climate variability (Mahmood et al., 2019). As CWT captures the amplitude of events at finer frequencies, its use in a bias correction approach enables the characterization of variability across all frequency resolutions. The algorithm of the CWBC is presented in Section 2, while Section 3 is dedicated to discussing the application of CWBC to bias correct sea surface temperature in Niño 3.4 region and Arctic sea-ice extent. Conclusions are presented in Section 4.

2. Materials and Methods

2.1. Systematic Bias in the Frequency Domain

The amplitude of an event at the associated frequency of the climate variable could be extracted using spectral density analysis. To understand the bias in amplitude and frequency, we generate two synthetic sine waves time series, $x(t) = A \sin(2\pi ft + \theta)$, exhibiting different amplitude (A), frequency (f), and phase (θ) (Figure 1a), for t forms 512 data points at a time increment of 0.25. The first time series represents observations (solid-black line), having a constant amplitude of 2.2 and frequency of 0.025, while the second time series represent the raw-model simulation (solid-blue line) having a constant amplitude of 1.2, frequency of 0.001, and 15° phase shift from the first time series. The spectral density, estimated using wavelet global power spectra, $\overline{W}^2(s)$ (details in Section 2.2), is shown in Figure 1b and represents the amplitude at the associated frequency of both sine waves.

Most bias correction approaches including DWBC correct for biases in the mean and standard deviation. After the application of DWBC, a mismatched frequency (Δf) can be seen as the gray-dashed line in Figure 1b. This is mainly due to the limited information on the frequency components obtained through DWT (defined only at dyadic frequencies).

2.2. Wavelet Analysis

Similar to DWT, CWT also disaggregates the time-frequency domain that characterizes the observed data; however, disaggregation occurs at finer frequencies creating a nearly continuous transformation. A CWT of a

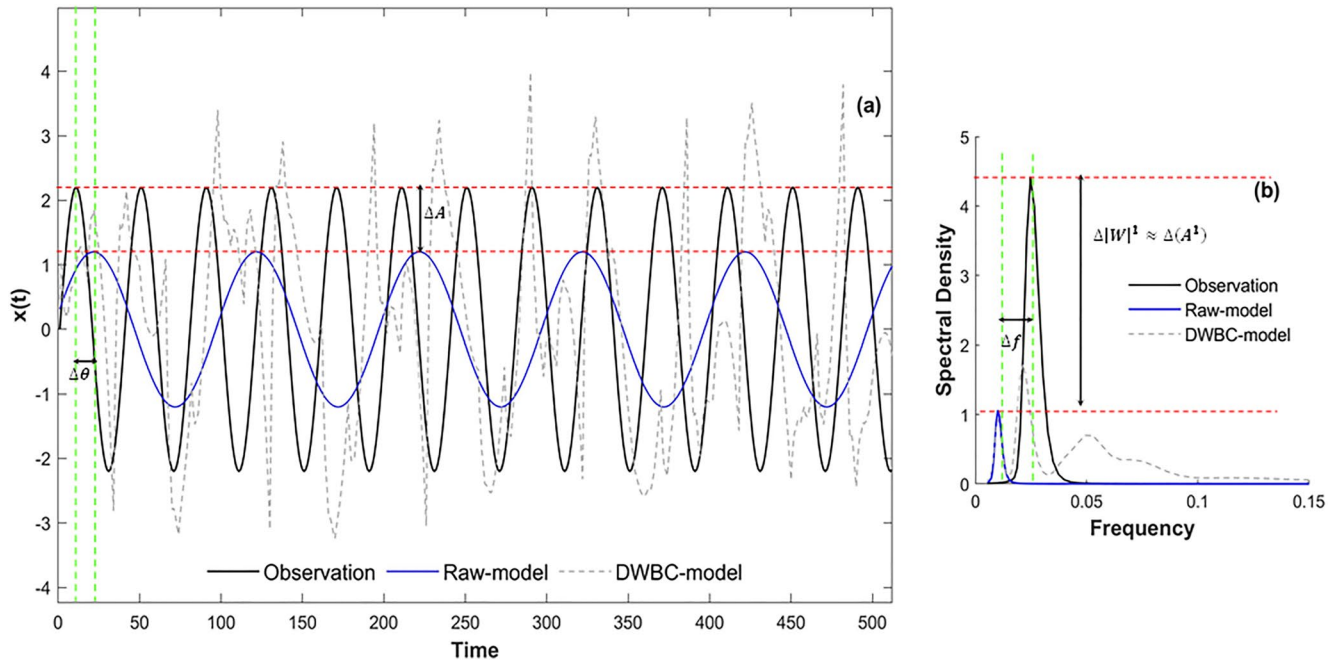


Figure 1. Illustration of bias in amplitude and frequency, and the limitation a discrete wavelet-based bias correction (DWBC) alternative presents when used for correction. (a) Two sine wave time series having different amplitude (A), and phase (θ), with one bias-corrected using DWBC. (b) The spectral density of the two time series before and after the application of DWBC.

discrete-time series, \mathbf{x}_t , is defined as the convolution of \mathbf{x}_t with a scale (s), and a translated version of a wavelet function, $\psi_0(\eta)$. As per the convolution theorem, the wavelet transform is the inverse of a Fourier transform as in Equation 1 (Torrence & Compo, 1998).

$$\mathbf{W}_t(s) = \sum_{k=0}^{T-1} \mathbf{x}_k \psi^*(s\omega_k) e^{i\omega_k t \delta t} \quad (1)$$

where ψ is the normalized wavelet mother function, $\psi_0(\eta)$, \mathbf{x}_k is a discrete Fourier transform as in Equation 2, $\mathbf{W}_t(s)$ is the wavelet coefficient, ω_k is the angular frequency defined in Equation 3, t is the time index, $k = 0 \dots T - 1$ is the frequency index, T is the number of points in the time series, and $*$ denotes the complex conjugate operator.

$$\mathbf{x}_k = \frac{1}{T} \sum_{t=0}^{T-1} \mathbf{x}_t e^{-2\pi i k t / T} \quad (2)$$

$$\omega_k = \begin{cases} \frac{2\pi k}{T \delta t}, & k \leq \frac{T}{2} \\ -\frac{2\pi k}{T \delta t}, & k > \frac{T}{2} \end{cases} \quad (3)$$

In general, the wavelet mother function, $\psi_0(\eta)$, is defined as a complex numbered function. Therefore, the wavelet transform, $\mathbf{W}_t(s)$, is also complex and the transformation can be divided into a real part, $\Re\{\mathbf{W}_t(s)\}$, and an imaginary part, $\Im\{\mathbf{W}_t(s)\}$, or, an amplitude, $|\mathbf{W}_t(s)|$, and phase, θ , $\tan^{-1} [\Im\{\mathbf{W}_t(s)\} / \Re\{\mathbf{W}_t(s)\}]$. Consequently, the wavelet power spectrum can be defined as $|\mathbf{W}_t(s)|^2$ and the time-averaged power spectra, better known as the global wavelet spectrum, are as defined in Equation 4.

$$\overline{\mathbf{W}}^2(s) = \frac{1}{T} \sum_{t=0}^T |\mathbf{W}_t(s)|^2 \quad (4)$$

where $|\mathbf{W}_t(s)|$ has been expressed as A in the following section for illustration purposes.

The mathematical concept of a wavelet transform, as a bandpass filter with a known response transform of the wavelet mother function, enables the reconstruction of time series either by deconvolution or the inverse filter. The reconstructed time series is then equal to the sum of real parts over all scales (Equation 5).

$$\mathbf{x}_t = \frac{\delta_j \delta t^{1/2}}{C_\delta \psi_0(\mathbf{0})} \sum_{j=0}^J \frac{\Re\{W_t(s_j)\}}{s_j^{1/2}} \quad (5)$$

For

$$s_j = s_0 2^{j\delta_j}, \quad j = 0, 1, \dots, J \quad (6)$$

$$J = \delta_j^{-1} \log_2(T\delta t/s_0) \quad (7)$$

where s_0 is the smallest resolvable scale, J is the largest scale, and C_δ is the reconstruction factor depends on the wavelet mother function (given in (Torrence & Compo, 1998)). In our experiment, we use the analytic Morlet wavelet mother function with a frequency resolution of δ_j as 0.1. Based on a sensitivity analysis, this frequency resolution was found adequate to match the current climate model simulations to the observation. Additional detail of wavelet mother functions used in CWT is presented in (Torrence & Compo, 1998).

2.3. Continuous-WBC (CWBC) Formulation

In the following, we denote the, \mathbf{x}^{oc} , \mathbf{x}^{rc} , and \mathbf{x}^{rf} as the time series representing observations, raw-current climate model simulations, and raw-future climate model simulations. The intent of any bias correction procedure is to form a model that maps \mathbf{x}^{rc} to \mathbf{x}^{oc} allowing the model to then transform \mathbf{x}^{rf} and determine the bias-corrected future. The CWBC formulation is based on the CWT described in Section 2.2 and aims to correct the bias illustrated in Figure 1 in both the amplitude of the spectrum as well as the phase. The following is the stepwise procedure to implement CWBC.

1. Preprocess the observation, \mathbf{x}^{oc} , raw-current, \mathbf{x}^{rc} , and raw-future, \mathbf{x}^{rf} , model simulations by removing seasonality or trend, if present. Set the seasonality or trend removed time series to have zero mean for observation, \mathbf{X}^{oc} , raw-current, \mathbf{X}^{rc} , and raw-future, \mathbf{X}^{rf} , model simulations.
2. Estimate the amplitude and phase of \mathbf{X}^{oc} , \mathbf{X}^{rc} , and \mathbf{X}^{rf} time-series using CWT. Let $A_i^{oc}(k)$ and $\theta_i^{oc}(k)$ as the amplitude and phase of \mathbf{X}^{oc} , $A_i^{rc}(k)$ and $\theta_i^{rc}(k)$ as the amplitude and phase of \mathbf{X}^{rc} , and $A_i^{rf}(k)$ and $\theta_i^{rf}(k)$ of \mathbf{X}^{rf} .
3. Map the amplitude and phase of each time series and estimate the bias correction factor for both amplitude, $\Delta A_i(k)$, and phase, $\Delta \theta_i(k)$, by taking the difference across time and frequency as in Equations 8 and 9.

$$\Delta A_i(k) = A_i^{oc}(k) - A_i^{rc}(k) \quad (8)$$

$$\Delta \theta_i(k) = \theta_i^{oc}(k) - \theta_i^{rc}(k) \quad (9)$$

4a. Bias correct $A_i^{rc}(k)$ and $\theta_i^{rc}(k)$ using Equations 8 and 9 to obtain the corrected amplitude, $\tilde{A}_i^{rc}(k)$, and phase, $\tilde{\theta}_i^{rc}(k)$, of \mathbf{X}^{rc} .

4b. Bias correct $A_i^{rf}(k)$ and $\theta_i^{rf}(k)$ using the same correction factors as the current climate in Equations 8 and 9 to obtain the corrected amplitude, $\tilde{A}_i^{rf}(k)$, and phase, $\tilde{\theta}_i^{rf}(k)$, of \mathbf{X}^{rf} as in Equations 10 and 11.

$$\tilde{A}_i^{rf}(k) = A_i^{rf}(k) + \Delta A_i(k) \quad (10)$$

$$\tilde{\theta}_i^{rf}(k) = \theta_i^{rf}(k) + \Delta \theta_i(k) \quad (11)$$

5a. Transform back $\tilde{A}_i^{rc}(k)$ and $\tilde{\theta}_i^{rc}(k)$ into the time domain using inverse wavelet transform on Equation 5 to obtain corrected amplitude and frequency of raw-current model simulation, $\tilde{\mathbf{X}}^{rc}$.

- 5b. Transform back $\tilde{A}_i^{jf}(k)$ and $\tilde{\theta}_i^{jf}(k)$ into the time domain using inverse wavelet transform on Equation 5 to obtain corrected amplitude and frequency of raw-future model simulation, \tilde{X}^{jf} .
6. Reintroduce the seasonality or trend and bias-corrected mean from step 1 to \tilde{X}^{rc} and \tilde{X}^{jf} to obtain the bias-corrected current, x^{rc} , and future, x^{jf} , model simulation.

3. Data and Applications

3.1. Data

The performance of CWBC is demonstrated using two climate variables—Niño 3.4 sea surface temperature (SST) and Arctic sea-ice extent. The monthly SST in Niño 3.4 region from 1870–2014 is a reconstructed SST time series retrieved from The Climate Data Guide: Nino SST Indices (Nino 1 + 2, 3, 3.4, 4; ONI and TNI) which is available at https://psl.noaa.gov/gcos_wgsp/Timeseries/Data/nino34.long.data. The SST Niño 3.4 used is based on the Hadley Centre Global Sea Ice and Sea Surface Temperature (HadISST) data set (Rayner et al., 2003) (hereafter, HadISST). For modeled data, we pick the historical and future climate r1i1p1f1 simulations of CAMS-CSM1-0 for representative concentration pathway (RCP) 2.6 (hereafter RCP2.6). Both data sets (hereafter, CAM-CSM1-0) are available on the CMIP6 website at <https://esgf-node.llnl.gov/search/cmip6/>.

The second variable used is the Arctic sea-ice extent (also used in (Kusumastuti et al., 2021)). The observed data of Arctic sea-ice extent in September from 1900–2010 is retrieved from the National Snow and Ice Data Center, National Aeronautics and Space Administration (NASA) of the USA. The current and future climate simulations are obtained from the fifth assessment report (AR5) of the Intergovernmental Panel on Climate Change, IPCC (Flato et al., 2014). The current climate spans from 1900 to 2010 in Figure 9.24 of AR5, IPCC, and the future climate spans from 2011 to 2100 in Figure TS.17 (Stocker et al., 2013) formed as the ensemble means of 37-CMIP5 models. Both data sets are available as 5 years-running mean of the raw variables.

Split-sample tests are conducted to test the model robustness. For Niño 3.4 sea surface temperature, the current period climate data is split into calibration (1870–1941) and validation periods (1942–2013). Similarly, for the Arctic sea-ice extent, the current climate data is split into calibration (1900–1955) and validation periods (1956–2009). The spectral densities of the calibration and validation periods are presented in Figures 2a and 2b for Niño 3.4 sea surface temperature and in Figures 2c and 2d for Arctic sea-ice extent. As anticipated, the model performs better in calibration in comparison to validation, and effectively bias corrects the magnitude and frequencies of events of both climate variables. As should be expected, the validation results, while not indicating a perfect match to the observations, do indicate the efficacy of the bias correction procedure that has been proposed. We do, however, note that it is advisable for the entire data record to be used to formulate the bias correction model, as a split-sample approach undertaken with limited data, is sub-optimal to when the entire data is used (Shen et al., 2022).

In the following sections, these two variables are bias-corrected using DWBC and CWBC. The results are then compared based on the power spectrum which is estimated using global wavelet power spectra. As described in Section 2.2, the wavelet power spectrum is equal to the power of wavelet coefficient, $|\mathcal{W}_t(s)|^2$, while the power spectrum in each frequency is equal to the global wavelet spectra or the time-averaged of $|\mathcal{W}_t(s)|^2$.

3.2. Niño 3.4 Sea Surface Temperature Simulations

The SST presented in the solid-black line in Figure 3a and the associated power spectrum in Figures 3b and 3c show strong power at three different frequencies of 0.025, 0.086, and 0.17. However, the raw CAM-CSM1-0 fails to simulate the second mode in the spectrum, indicating high power at two different frequencies of 0.03 and 0.16.

The power spectrum of DWBC bias-corrected CAM-CSM1-0 series is represented by the dashed-blue line in Figure 3b. The spectrum exhibits a large correction in amplitude in both the first and third dominant frequencies in the current climate. On the other hand, the power spectrum of CWBC bias-corrected series removes the biases in the amplitude as well as the frequency, as shown in the dashed-green line of Figure 3c. The results suggest

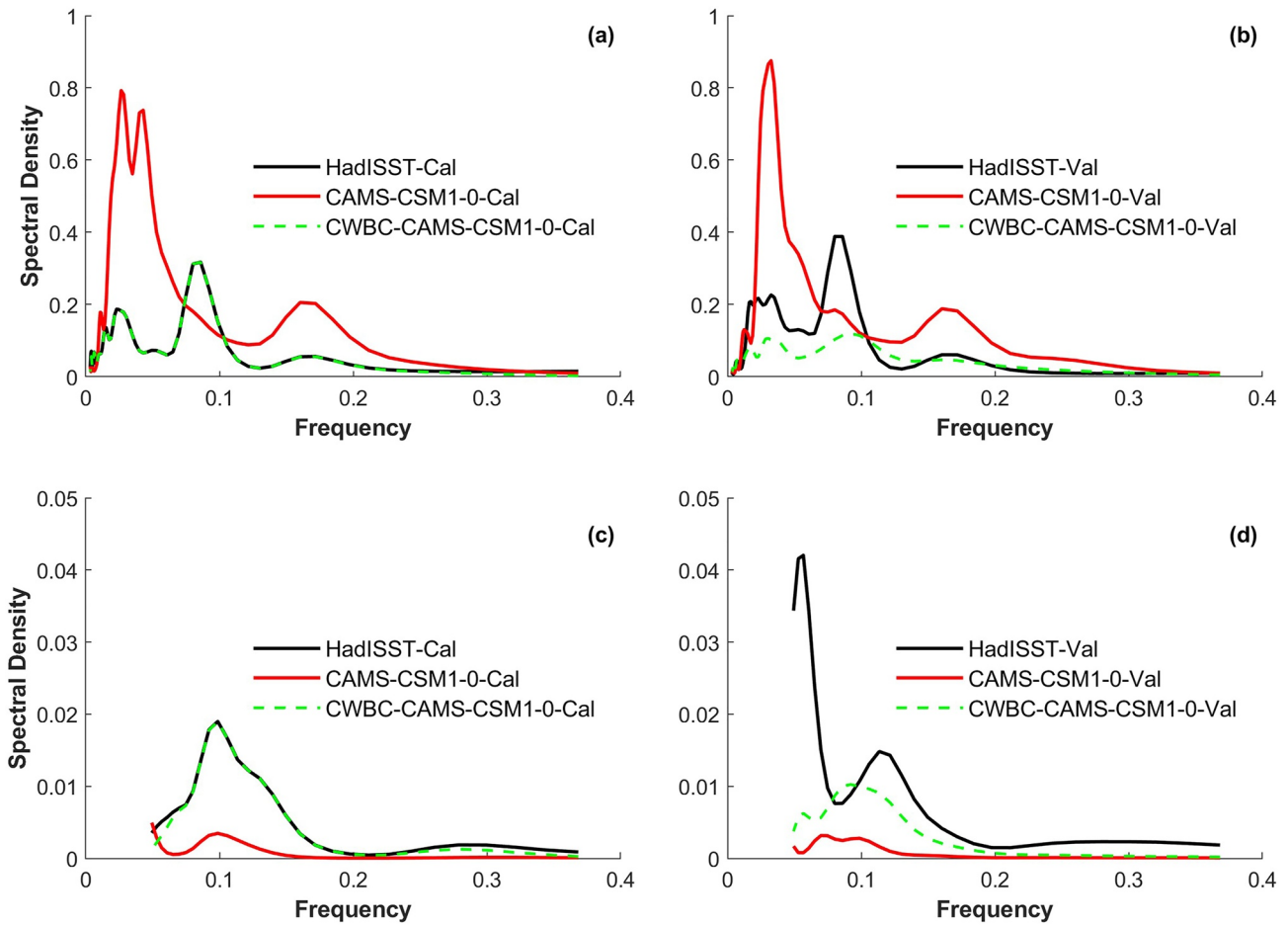


Figure 2. Spectral density of the calibration period of (a) Niño 3.4 sea surface temperature and (b) Arctic sea-ice extent and the validation period of (c) Niño 3.4 sea surface temperature and (d) Arctic sea-ice extent.

that CWBC outperforms DWBC by matching the observed amplitude and frequency in the current climate. As the correction factor remains unchanged for the future, the corrected CAM-CSM1-0 is expected to retain the frequency information of the raw-future data after correction.

3.3. Arctic Sea-Ice Extent Simulations

The Arctic sea-ice extent in September as shown in Figure 4, exhibits a significant decreasing trend that is projected until 2100. The current observed time series shows high amplitudes at three different frequencies of 0.03, 0.057, and 0.12. On the other hand, the ensemble mean of raw CMIP5 simulations underestimates the magnitude of events across the time series as well as fails to simulate the three frequencies components by indicating strong amplitudes at different frequencies 0.037 and 0.099.

Although DWBC significantly corrects for the biases in the power of sea-ice extent time series in the current climate (Figure 4b), it is unable to match the representation of the observed frequencies, a mathematical limitation that was noted in the illustrative example in Figure 1. The bias correction of the amplitude of future sea-ice extent shows an unrealistic strong power at a higher frequency (Figure 4d). On the other hand, the application of CWBC shows significant improvements in representing both amplitude and frequencies (Figure 4c). The power spectrum of sea-ice extent in the current climate matches with that observed while for the future climate (Figure 4e), it demonstrates a correction that is different from what the DWBC approach presents.

It is worth noting that the Arctic sea-ice extent data set exhibits a significant decreasing trend since 1900 and is predicted to continue until 2100. In the application of CWBC, the bias in trend is corrected using the proposed

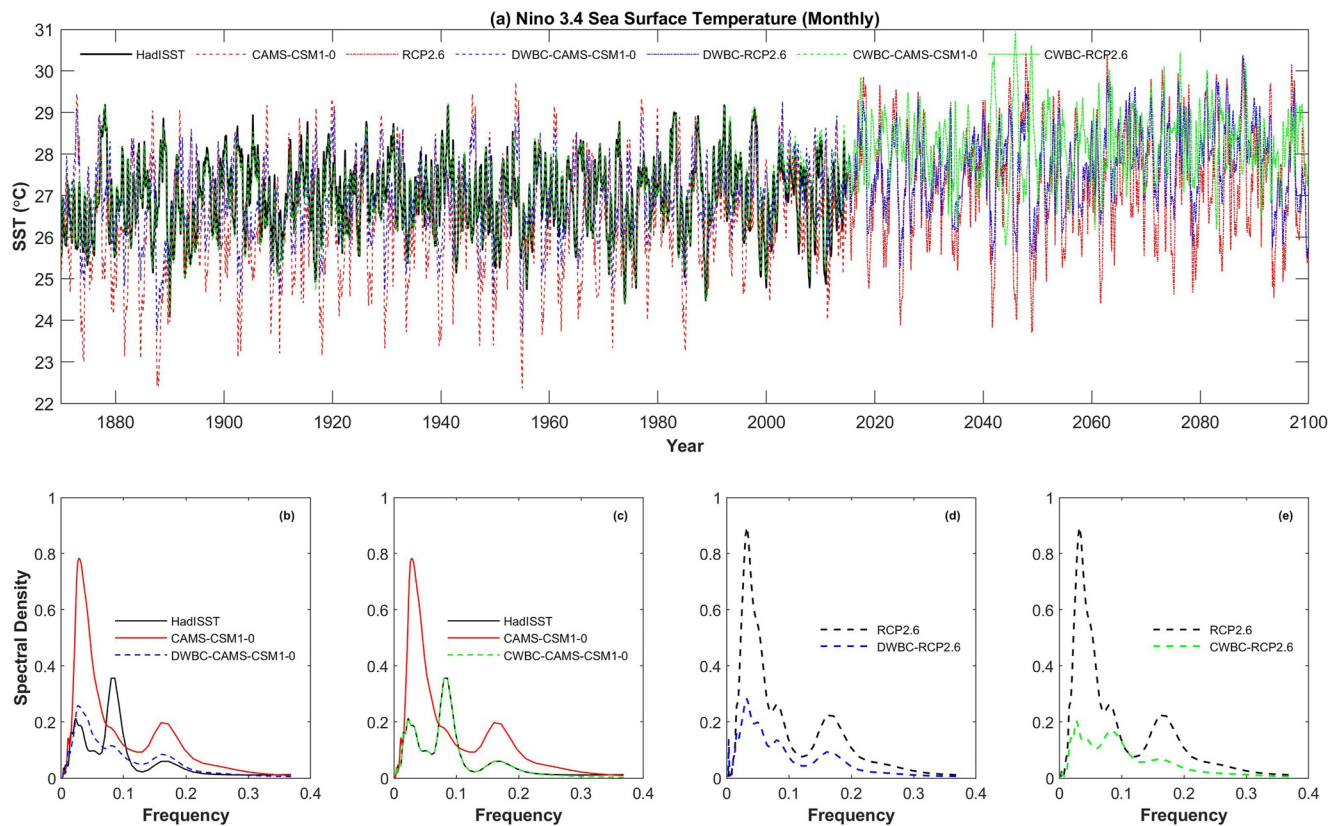


Figure 3. Reconstructed, raw, and bias-corrected sea surface temperature (SST)-Niño 3.4 region (a); spectral density of observed, raw, and discrete wavelet-based bias correction (DWBC)-SST (b) and continuous wavelet-based bias correction (CWBC)-SST (c) for current climate; spectral density of raw SST of the current climate for RCP2.6 projection, and the DWBC-SST (d), and CWBC-SST (e).

method in DWBC (Kusumastuti et al., 2021). The delta factor presented in Equations 9 and 10 in the paper is adopted in CWBC to maintain the continuity from the current to future climate. Therefore, as can be observed in Figure 4a, both DWBC and CWBC bias correct the trend in the current climate with respect to observation while maintaining it to the future climate.

4. Conclusions

A novel time-frequency domain approach for correcting biases in the magnitude and frequency of the events of climate model simulations is developed. To illustrate the utility of the approach and the implications of the correction logic to the power spectrum of the data, an example using two sine waves with different amplitudes and phases is presented. The discrete wavelet transform-based bias correction alternatives were demonstrated to be less effective in modeling non-dyadic frequencies leading to a possible mismatch in both the amplitude (or power) and the frequencies of the variables of interest. The continuous wavelet transform-based bias correction approach proposed here operates across a near-continuous frequency domain and is, therefore, able to identify the biases at non-dyadic frequencies as well.

The capability of CWBC is demonstrated using two climate variable time series—Niño 3.4 SST and Arctic sea-ice extent. These represent climate series that exhibit an obvious pattern of recurrence and trend. The application of two bias correction approaches shows that the fine resolution spectrum obtained through the CWT procedure ensures that the complete spectrum is well characterized and corrected for any systematic biases. The finer scale biases are missed out by other alternatives such as QM or DWT. The finer scale variability in a climate series plays an important role in characterizing the low frequency climatic phenomena, for example, the Pacific Decadal Oscillation, the Madden-Julian Oscillation, and the North Atlantic Oscillation amongst others.

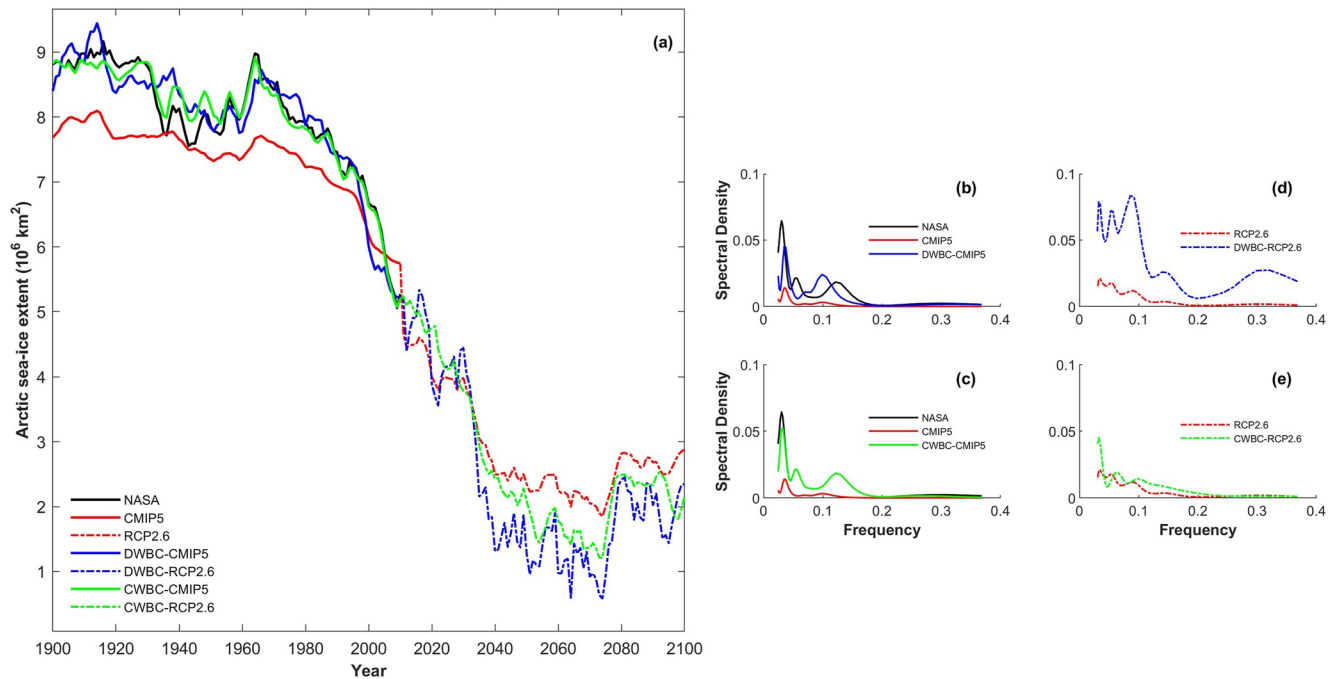


Figure 4. Five-year running mean of observed, raw, discrete wavelet-based bias correction (DWBC)-, and continuous wavelet-based bias correction (CWBC)-, September Arctic sea-ice extent for the current climate and future climate for RCP2.6 projection (a); the spectral density of observed, raw-, and DWBC- (b), and CWBC- (c) of current climate; the spectral density of raw-, and DWBC- (d), and CWBC- (e) of future climate for RCP2.6 projection.

Data Availability Statement

The SST observation data sets are available at https://psl.noaa.gov/gcos_wgsp/Timeseries/Data/nino34.long.data while the monthly historical and future climate r11p1f1 simulations of CAMS-CSM1-0 for representative concentration pathway (RCP) 2.6 is available at <https://esgf-node.lnl.gov/search/cmip6/>. The Arctic sea-ice extent data is available at <https://sos.noaa.gov/datasets/sea-ice-extent-arctic-only-1850-present/>. The data used in Figure 4a. is extracted from Figure 9.24 of AR5, IPCC (Flato et al., 2014), and Figure TS.17 (Stocker et al., 2013).

Acknowledgments

We acknowledge the World Climate Research Programme's Working Group on Coupling Modelling, which responsible for CMIP, the climate data guide website to make the Niño 3.4 SST data sets are available, National Snow and Ice Data Center, National Aeronautics and Space Administration (NASA) of the U.S. to make the Arctic sea-ice extent data is available. The first author would also like to acknowledge the financial support from the Directorate of Resources, Directorate General of Higher Education, Ministry of Education, Culture, Research, and Technology of The Republic of Indonesia. Partial support for this research came from Australian research Council Discovery Project DP180102737. Open access publishing facilitated by University of New South Wales, as part of the Wiley – University of New South Wales agreement via the Council of Australian University Librarians.

References

- Abramovich, F., Bailey, T. C., & Sapatinas, T. (2000). Wavelet analysis and its statistical applications. *Journal of the Royal Statistical Society: Series D (The Statistician)*, 49(1), 1–29. <https://doi.org/10.1111/1467-9884.00216>
- Adamowski, K., Prokoph, A., & Adamowski, J. (2009). Development of a new method of wavelet aided trend detection and estimation. *Hydrological Processes*, 23(18), 2686–2696. <https://doi.org/10.1002/hyp.7260>
- Adarsh, S., & Janga Reddy, M. (2015). Trend analysis of rainfall in four meteorological subdivisions of southern India using nonparametric methods and discrete wavelet transforms. *International Journal of Climatology*, 35(6), 1107–1124. <https://doi.org/10.1002/joc.4042>
- Beadling, R. L., Russell, J. L., Stouffer, R. J., Mazloff, M., Talley, L. D., Goodman, P. J., et al. (2020). Representation of southern ocean properties across coupled model Intercomparison Project generations: CMIP3 to CMIP6. *Journal of Climate*, 33(15), 6555–6581. <https://doi.org/10.1175/jcli-d-19-0970.1>
- Bollasina, M. A., & Ming, Y. (2013). The general circulation model precipitation bias over the southwestern equatorial Indian Ocean and its implications for simulating the South Asian monsoon. *Climate Dynamics*, 40(3), 823–838. <https://doi.org/10.1007/s00382-012-1347-7>
- Brunner, M. I., & Gilleland, E. (2020). Stochastic simulation of streamflow and spatial extremes: A continuous, wavelet-based approach. *Hydrology and Earth System Sciences*, 24(8), 3967–3982. <https://doi.org/10.5194/hess-24-3967-2020>
- Fan, X., Miao, C., Duan, Q., Shen, C., & Wu, Y. (2020). The performance of CMIP6 versus CMIP5 in simulating temperature extremes over the global land surface. *Journal of Geophysical Research: Atmospheres*, 125(18), e2020JD033031. <https://doi.org/10.1029/2020JD033031>
- Flato, G., Marotzke, J., Abiodun, B., Braconnot, P., Chou, S. C., Collins, W., et al. (2014). Evaluation of climate models. In *Climate change 2013: The physical science basis. Contribution of working group I to the fifth assessment report of the intergovernmental Panel on climate change* (pp. 741–866). Cambridge University Press.
- Haerter, J. O., Hagemann, S., Moseley, C., & Pianì, C. (2011). Climate model bias correction and the role of timescales. *Hydrology and Earth System Sciences*, 15(3), 1065–1079. <https://doi.org/10.5194/hess1510652011>
- Jiang, Z., Rashid, M. M., Johnson, F., & Sharma, A. (2021). A wavelet-based tool to modulate variance in predictors: An application to predicting drought anomalies. *Environmental Modelling & Software*, 135, 104907. <https://doi.org/10.1016/j.envsoft.2020.104907>
- Jiang, Z., Sharma, A., & Johnson, F. (2020). Refining predictor spectral representation using wavelet soft for improved natural system modeling. *Water Resources Research*, 56(3), e2019WR026962. <https://doi.org/10.1029/2019wr026962>

- Jiang, Z., Sharma, A., & Johnson, F. (2021). Variable transformations in the spectral domain—Implications for hydrologic forecasting. *Journal of Hydrology*, 603, 126816. <https://doi.org/10.1016/j.jhydrol.2021.126816>
- Johnson, F., & Sharma, A. (2011). Accounting for interannual variability: A comparison of options for water resources climate change impact assessments. *Water Resources Research*, 47(4). <https://doi.org/10.1029/2010wr009272>
- Johnson, F., & Sharma, A. (2012). A nesting model for bias correction of variability at multiple time scales in general circulation model precipitation simulations. *Water Resources Research*, 48(1). <https://doi.org/10.1029/2011wr010464>
- Kusumastuti, C., Jiang, Z., Mehrotra, R., & Sharma, A. (2021). A signal processing approach to correct systematic bias in trend and variability in climate model simulations. *Geophysical Research Letters*, 48(13), e2021GL092953. <https://doi.org/10.1029/2021GL092953>
- Li, H., Sheffield, J., & Wood, E. F. (2010). Bias correction of monthly precipitation and temperature fields from Intergovernmental Panel on Climate Change AR4 models using equidistant quantile matching. *Journal of Geophysical Research*, 115(D10), D10101. <https://doi.org/10.1029/2009jd012882>
- Lin, R., Zhu, J., & Zheng, F. (2019). The application of the SVD method to reduce coupled model biases in seasonal predictions of rainfall. *Journal of Geophysical Research: Atmospheres*, 124(22), 11837–11849. <https://doi.org/10.1029/2018JD029927>
- Maheswaran, R., & Khosa, R. (2012). Comparative study of different wavelets for hydrologic forecasting. *Computers & Geosciences*, 46, 284–295. <https://doi.org/10.1016/j.cageo.2011.12.015>
- Mahmood, R., Jia, S., & Zhu, W. (2019). Analysis of climate variability, trends, and prediction in the most active parts of the Lake Chad basin, Africa. *Scientific Reports*, 9(1), 6317. <https://doi.org/10.1038/s41598-019-42811-9>
- Mehrotra, R., & Sharma, A. (2012). An improved standardization procedure to remove systematic low frequency variability biases in GCM simulations. *Water Resources Research*, 48(12). <https://doi.org/10.1029/2012wr012446>
- Mehrotra, R., & Sharma, A. (2015). Correcting for systematic biases in multiple raw GCM variables across a range of timescales. *Journal of Hydrology*, 520, 214–223. <https://doi.org/10.1016/j.jhydrol.2014.11.037>
- Mehrotra, R., & Sharma, A. (2019). A resampling approach for correcting systematic spatiotemporal biases for multiple variables in a changing climate. *Water Resources Research*, 55(1), 754–770. <https://doi.org/10.1029/2018WR023270>
- Mehrotra, R., Sharma, A., Bari, M., Tuteja, N., & Amirthanathan, G. (2014). An assessment of CMIP5 multi-model decadal hindcasts over Australia from a hydrological viewpoint. *Journal of Hydrology*, 519, 2932–2951. <https://doi.org/10.1016/j.jhydrol.2014.07.053>
- Nguyen, H., Mehrotra, R., & Sharma, A. (2016). Correcting for systematic biases in GCM simulations in the frequency domain. *Journal of Hydrology*, 538, 117–126. <https://doi.org/10.1016/j.jhydrol.2016.04.018>
- Nourani, V., Danandeh Mehr, A., & Azad, N. (2018). Trend analysis of hydroclimatological variables in Urmia lake basin using hybrid wavelet Mann–Kendall and Şen tests. *Environmental Earth Sciences*, 77(5), 207. <https://doi.org/10.1007/s12665-018-7390-x>
- Ojha, R., Kumar, D. N., Sharma, A., & Mehrotra, R. (2013). Assessing severe drought and wet events over India in a future climate using a nested bias-correction approach. *Journal of Hydrologic Engineering*, 18(7), 760–772. [https://doi.org/10.1061/\(asce\)he.1943-5584.0000585](https://doi.org/10.1061/(asce)he.1943-5584.0000585)
- Randall, D. A., Wood, R. A., Bony, S., Colman, R., Fichefet, T., Fyfe, J., et al. (2007). Climate models and their evaluation. In *Climate change 2007: The physical science basis. Contribution of working group I to the fourth assessment report of the intergovernmental Panel on climate change* [In S. Solomon, D. Qin, M. Manning, Z. Chen, M. Marquis, K. B. Averyt, et al. (eds.)] (pp. 589–662). Cambridge University Press.
- Rashid, M. M., Johnson, F., & Sharma, A. (2018). Identifying sustained drought anomalies in hydrological records: A wavelet approach. *Journal of Geophysical Research: Atmospheres*, 123(14), 7416–7432. <https://doi.org/10.1029/2018jd028455>
- Rashid, M. M., Sharma, A., & Johnson, F. (2020). Multi-model drought predictions using temporally aggregated climate indicators. *Journal of Hydrology*, 581, 124419. <https://doi.org/10.1016/j.jhydrol.2019.124419>
- Rayner, N. A., Parker, D. E., Horton, E. B., Folland, C. K., Alexander, L. V., Rowell, D. P., & Kaplan, A. (2003). Global analyses of sea surface temperature, sea ice, and night marine air temperature since the late nineteenth century. *Journal of Geophysical Research*, 108(D14), 4407. <https://doi.org/10.1029/2002JD002670>
- Sang, Y.-F., Wang, Z., & Liu, C. (2013). Discrete wavelet-based trend identification in hydrologic time series. *Hydrological Processes*, 27(14), 2021–2031. <https://doi.org/10.1002/hyp.9356>
- Shen, H., Tolson, B. A., & Mai, J. (2022). Time to update the split-sample approach in hydrological model calibration. *Water Resources Research*, 58(3), e2021WR031523. <https://doi.org/10.1029/2021WR031523>
- Stocker, T. F., Qin, D., Plattner, G.-K., Alexander, L. V., Allen, S. K., Bindoff, N. L., et al. (2013). Technical summary. In *Climate change 2013: The physical science basis. Contribution of working group I to the fifth assessment report of the intergovernmental Panel on climate change* (pp. 33–115). Cambridge University Press.
- Teutschbein, C., & Seibert, J. (2013). Is bias correction of regional climate model (RCM) simulations possible for non-stationary conditions? *Hydrology and Earth System Sciences*, 17(12), 5061–5077. <https://doi.org/10.5194/hess-17-5061-2013>
- Torrence, C., & Compo, G. P. (1998). A practical guide to wavelet analysis. *Bulletin of the American Meteorological Society*, 79(1), 61–78. [https://doi.org/10.1175/1520-0477\(1998\)079<0061:apgtwa>2.0.co;2](https://doi.org/10.1175/1520-0477(1998)079<0061:apgtwa>2.0.co;2)
- Trauth, M. H., Bookhagen, B., Marwan, N., & Strecker, M. R. (2003). Multiple landslide clusters record Quaternary climate changes in the northwestern Argentine Andes. *Palaeogeography, Palaeoclimatology, Palaeoecology*, 194(1), 109–121. [https://doi.org/10.1016/S0031-0182\(03\)00273-6](https://doi.org/10.1016/S0031-0182(03)00273-6)
- Wang, Z., Han, L., Zheng, J., Ding, R., Li, J., Hou, Z., & Chao, J. (2021). Evaluation of the performance of CMIP5 and CMIP6 models in simulating the Victoria Mode?El Niño relationship. *Journal of Climate*, 34(18), 7625–7644. <https://doi.org/10.1175/jcli-d-20-0927.1>
- Wood, A. W., Leung, L. R., Sridhar, V., & Lettenmaier, D. P. (2004). Hydrologic implications of dynamical and statistical approaches to downscaling climate model outputs. *Climatic Change*, 62(1), 189–216. <https://doi.org/10.1023/B:CLIM.0000013685.99609.9e>